Optimization of transparent conducting Al-doped zinc oxide filmsprepared by pulsed laser deposition

AGURA Hideaki, SUZUKI Akio, MATSUSHITA Tatsuhiko and AOKI Takanori

Abstract

Approximately 100-nm-thick Al-doped zinc oxide (AZO) films with 100-500 stacking layers have been prepared on glass substrate at 230℃ by pulsed laser deposition (PLD) using a split target divided into AZO (Al_2O_3 : 1wt.%) and AZO (Al_2O_3 : 2wt.%). Film compositions were adjusted by changing the ratio (trace ratio) of the time required to irradiate each side of the target alternately by an ArF excimer laser (λ = 193nm) or Nd: YAG laser (λ =266,355 and 532nm). As a result, the AZO film with 500 stacking layers deposited by irradiating pulsed laser beam of the wavelength of 193nm at repetition frequency of 2 Hz gave the lowest resistivity of $2.24\times10^{-4}\Omega\cdot$cm under optimized conditions of laser energy density of 1 J/cm^2 and trace ratio of AZO (Al_2O_3 : 1wt.%) : (Al_2O_3 : 2wt.%) = 1 : 4. The surface roughness was 0.69nm and the FWHM of the ZnO(0002) peak was 0.73°. An average transmittance of more than 90% in the visible range were obtained for the AZO films with 500 stacking layers deposited under these optimized conditions, providing useful functionality as TCO films in the visible range.

Keywords

Al-doped zinc oxide film; pulsed laser deposition; transparent conducting oxide

1. Introduction

Recently, a great deal of interest has turned to transparent conducting oxide (TCO) films based on a zinc oxide (ZnO) system because of its advantages such as non-toxicity and cheapness [1-4]. ZnO is one of the promising wide-band-gap (about 3.37 eV) semiconductor, for use in the preparation of ultraviolet and visible light-emitting devices [5-6]. It has recently attracted attention because of applications such as nano-wires and nano-rods for observing quantum effects [7] and for fabrication of field-effect transistors [8]. We have fabricated TCO films with Ga-doped ZnO grown using SHG of Nd:YAG laser (λ

Received March 13, 2006.

Department of Electronics, Information and Communication Engineering, Osaka Sangyo University, 3-1-1 Nakagaito, Daito, Osaka 574-8530, Japan

=532nm) and have tried to utilize the zinc oxide film as a transparent electrode of solar cells [3].

ZnO films, if utilized for TCO electrodes, are superior to ITO films from the viewpoint of transparency in the visible wavelength region [9-13]. Moreover, Al-doped ZnO (AZO) films fabricated by the PLD method [2, 4] having the advantage of the ability to reproduce the target compositions [14] and the sputtering method [15-17] present excellent high transparency and low resistivity properties. Focusing on this theme, our group conducted a trial fabrication of AZO films by a pulsed laser deposition (PLD) method using a split target divided into two parts of AZO (Al_2O_3 : 1 wt.%) and AZO (Al_2O_3 : 2wt.%), which resulted in the adjustment of film composition by changing the ratio (trace ratio) of the time required to irradiate each side of the target alternately by a Nd:YAG laser (λ =266, 355 and 532nm) or an ArF excimer laser (λ =193nm). In this paper, structural, electrical and optical properties of AZO films with approximately 100-nm-thick, fabricated by trying to make the number of laminated layer of films most suitable are described.

2. Experimental

AZO films were prepared by the PLD system as shown in Fig. 1 under conditions listed in Table 1. AZO films were deposited on Corning #7059 glass substrates with an area of 38

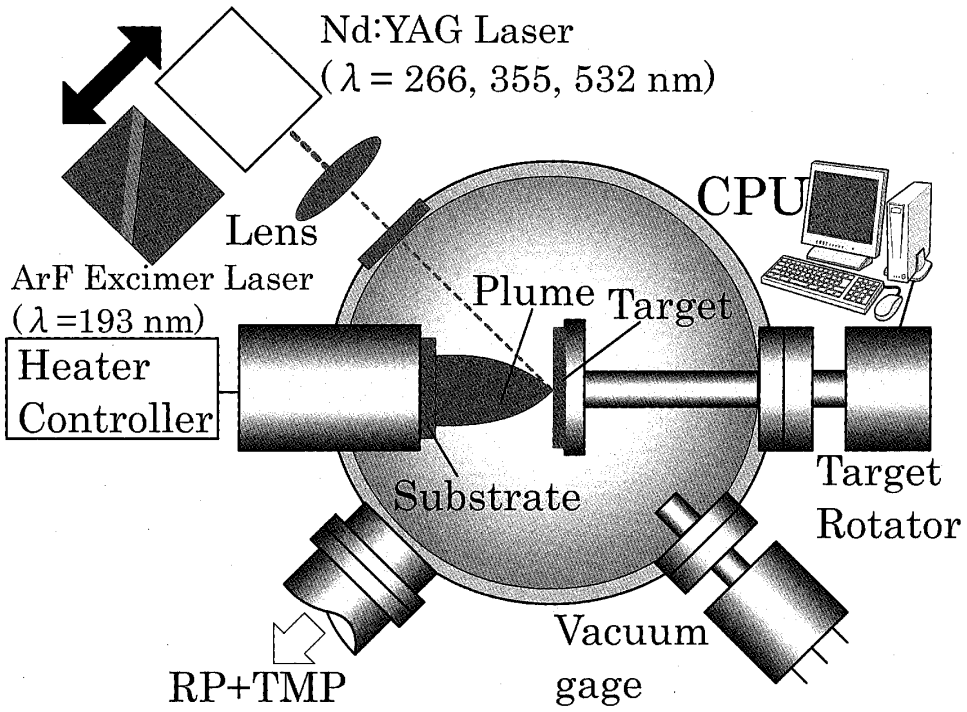

Fig. 1. Illustration of pulsed laser deposition system for AZO films using Nd: YAG laser and ArF excimer laser.

Table 1. Preparation conditions for AZO films.

Laser (λ = 193, 266, 355, 532 nm)	Laser Energy	40, 100 mJ
	Repetition Frequency	2, 10 Hz
	Laser Energy Density	1, 2.5 J/cm^2
Chamber	Target	AZO (1 wt.% Al_2O_3) AZO (2 wt.% Al_2O_3) (Split)
	Substrate	Corning #7059
	Target to Substrate Distance	40 mm
	Substrate Temperature	230 ℃
	Base Pressure	~ 10^{-4} Pa
Film Thickness		100 nm

×26 mm by irradiating a Nd:YAG laser (Spectra-Physics, PRO-350, λ=266, 355 and 532 nm) or an ArF excimer laser (LAMBDA PHYSIK, COMPex102, λ=193nm), adjusted to provide an energy density of 2.5 J/cm^2. The diameter of laser beam was reduced to one twentieth through a quartz lens. A substrate temperature of 230 °C was set, considering preliminary experimental results. The target was rotated during laser irradiation using a pulsed motor controlled by a personal computer, to avoid the formation of deep craters that affect material ejection. The film thickness was measured using a stylus instrument (KLA TENCOR, P-10). The resistivity, carrier concentration and Hall mobility were measured by the van der Pauw method (BIO-RAD, HL5500PC). Transmittance through the films, with Corning #7059 glass as a reference, was measured in the wavelength range from 300-2500 nm using a spectrophotometer (Hitachi, U-3500). The cross-section and surface morphology of the films were observed using a high-resolution field emission scanning electron microscope (FE-SEM) (Hitachi, S-4700) and an atomic force microscope (AFM) (Topometrix, TMX-2000). The crystal orientation was evaluated by X-ray diffraction using CuK α radiation (Shimadzu, XRD-6100) with the θ-2θ method. The film structure was analyzed by a high-resolution field emission transmission electron microscope (FE-TEM) (Hitachi, HF-2000).

3. Results and discussion

3-1 Variation in characteristics of films fabricated with various laser wavelengths

With various laser beam wavelengths keeping the laser energy density at a constant value of 2.5 J/cm^2, AZO films have been deposited on glass substrates by stacking alternate layers with a trace ratio of AZO (1 wt.%) : AZO (2 wt.%) = 1 : 1 (namely, AZO (1.5 wt.%)) and a target-to-substrate distance of 40 mm. The film thickness was approximately 100 nm.

Fig. 2 shows the transmittance spectra for the AZO films with 100 layers. As the wavelength of the laser beam began to be shortening, the transmittance in the wavelength region above 1000 nm started to reduce. In the visible range (400-700 nm), the average transmittance was more than 85 % for the films deposited with shorter wavelength (193-355 nm) laser beam, but was clearly less for the film deposited with a laser beam wavelength of 532nm.

The electrical properties for AZO films grown under these conditions are shown in Table 2. As the wavelength of the laser beam decreased from 532 to 193 nm, it was found that the resistivity ρ decreased from 13.3×10^{-4} to 3.64×10^{-4} $\Omega\cdot$cm and the Hall mobility μ increased from 17.2 to 21.6 $cm^2/V\cdot s$. On the other hand, the aluminum content was quantitatively determined using the energy dispersion spectroscopy (EDS) method: the aluminum content of 1.58 wt.%, 0.97 wt.%, 0.32 wt.% and 0.1 wt.% was obtained for the films grown at the wavelength of 193 nm, 266 nm, 355 nm and 532 nm, respectively. From these results, it was considered that as the wavelength used for laser ablation increased, the decrease of carrier concentration due to the decreased aluminum content was caused.

Fig. 3 shows FE-SEM and AFM micrographs of the surfaces of AZO films fabricated at laser beam wavelengths of (a) 193, (b) 266, (c) 355 and (d) 532 nm. The FE-SEM images

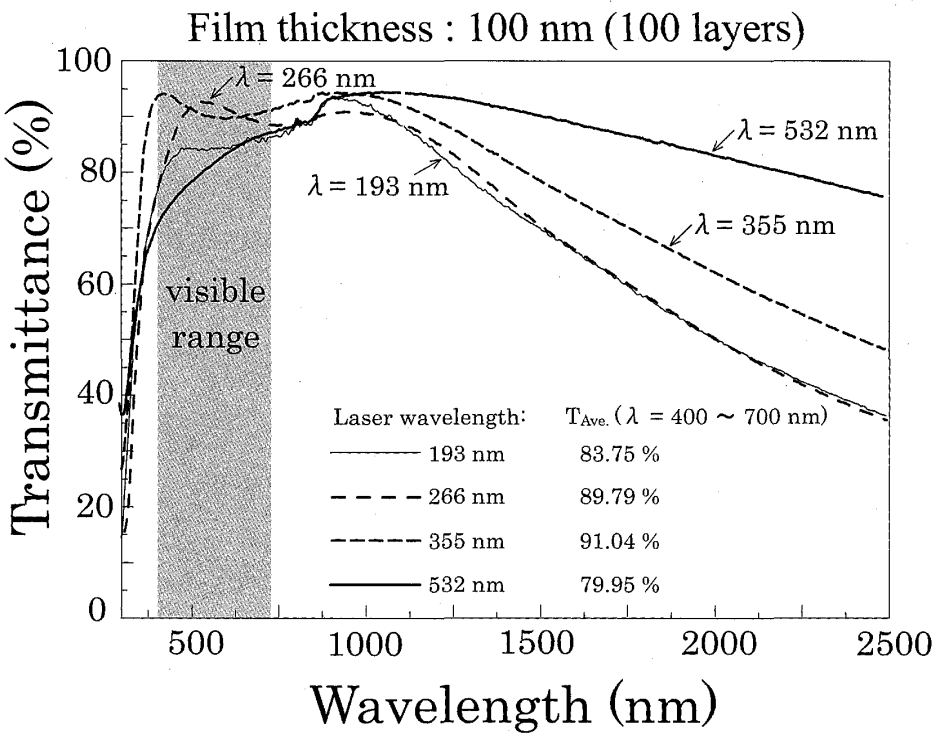

Fig. 2. Optical transmittance spectra of 100-nm-thick AZO films (100 layers) deposited with various wavelengths (193-532nm).

Table 2. Electrical properties of AZO films (100 layers) grown with various wavelengths.
Film Thickness: 100nm

Wavelength λ (nm)	Resistivity ρ ($\times 10^{-4}$ $\Omega \cdot$cm)	Hall Mobility μ ($cm^2/V \cdot s$)	Carrier Concentration n ($\times 10^{20}$ cm^{-3})
532	13.3	17.2	2.72
355	7.02	14.8	6.00
266	5.82	16.9	6.34
193	3.64	21.6	7.94

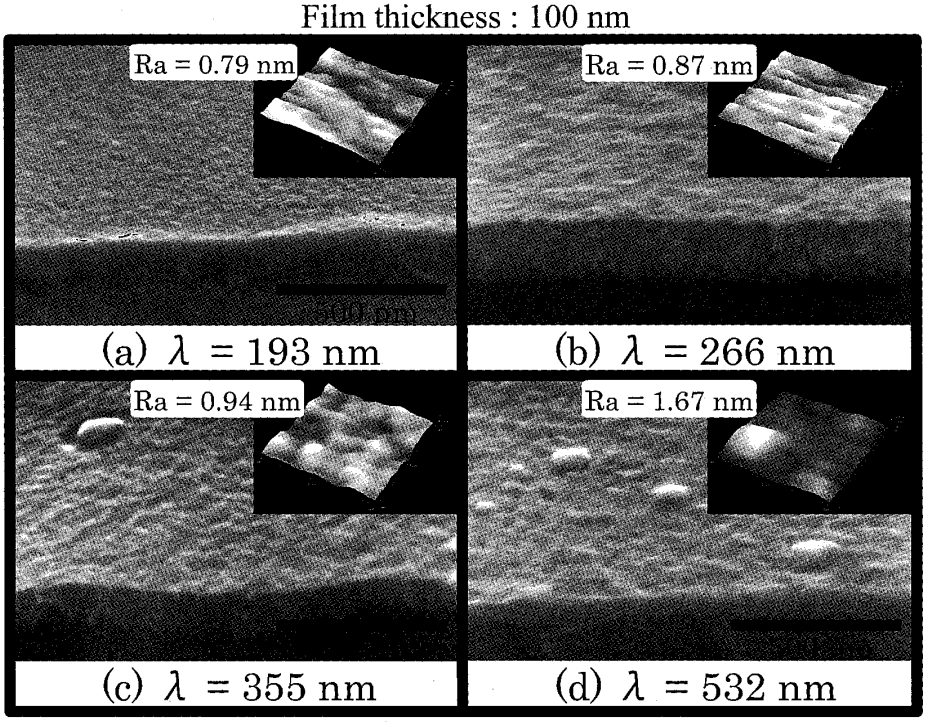

Fig. 3. FE-SEM and AFM images for the surfaces of AZO films (100 layers) deposited with varied wavelengths (193-532 nm).

showed that droplets were more easily generated as the wavelength of the laser beam increased. Especially, there was a clear distinction between the surface of films deposited at a wavelength of 532 nm and the others, namely, in Fig. 3 (d) the surface of this film appeared molten as well as having many droplets. Similarly, the surface roughness obtained from AFM images, shown in the insets, became coarser from 0.79 to 1.67 nm as the wavelength of the laser beam increased from 193 to 532 nm.

From these results, it was found that as the wavelength of laser beam used in deposition increased, the deterioration of electrical properties of AZO films was caused as shown in Table 2. To confirm this assumption from the viewpoint of the structural properties of the AZO films, XRD measurements and FE-SEM observations were performed. Fig. 4 shows

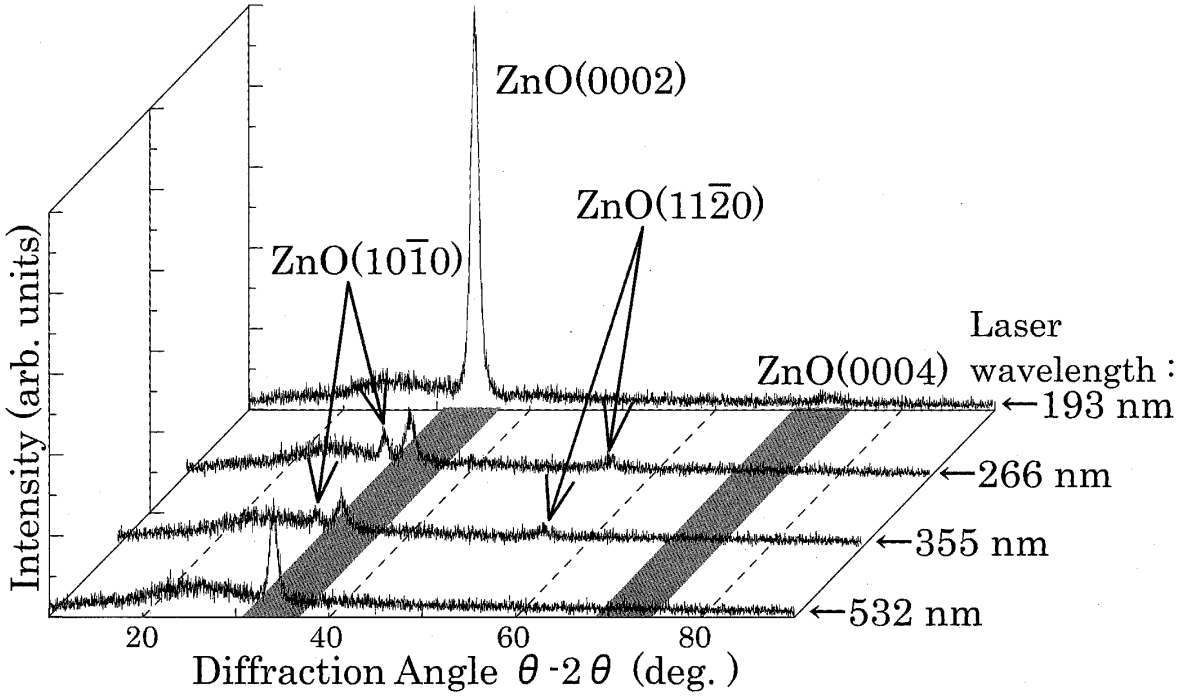

Fig. 4. XRD spectra obtained by the θ-2θ method for 100-nm-thick AZO films (100 layers) grown by varied wavelengths (193-532 nm).

the laser beam-wavelength-dependence of the XRD spectra of the films obtained by the θ-2θ method. For a wavelength of 193 nm, strong (0002) (θ = 34.42°) and weak (0004) (θ = 72.56°) facets could be identified in the diffraction spectra with the c-axis orientation. Next, for wavelengths of 266 and 355 nm, weak (10-10) (θ = 31.77°) and (11-20) (θ = 56.60°) peaks, suggestive of polycrystalline properties of AZO films, were identified in addition to an weak (0002) peak with the c-axis orientation. However, for a wavelength of 532 nm, a strong (0002) peak again appeared, which implied that the component with the c-axis orientation was partially included in the large grains created due to the thermal effect, as observed in Fig. 3 (d).

Fig. 5 shows FE-TEM images obtained for the AZO films deposited with laser beam wavelengths of (a) 193, (b) 266, (c) 355 and (d) 532 nm. As can be seen in Fig. 5 (a), for a wavelength of 193 nm, the crystal lattice was regularly aligned on the surface of the AZO film. Also, for a wavelength of 266 nm, shown in Fig. 5 (b), regularity of the crystal lattice was well preserved, as in Fig. 5 (a). On the other hand, for wavelengths of 355 nm, in Fig. 5 (c) and 532 nm, in Fig. 5 (d), only local regularity in the crystal growth emerged from different points in the film.

3.2 Variation of the characteristics of films by changing the number of stacking layers

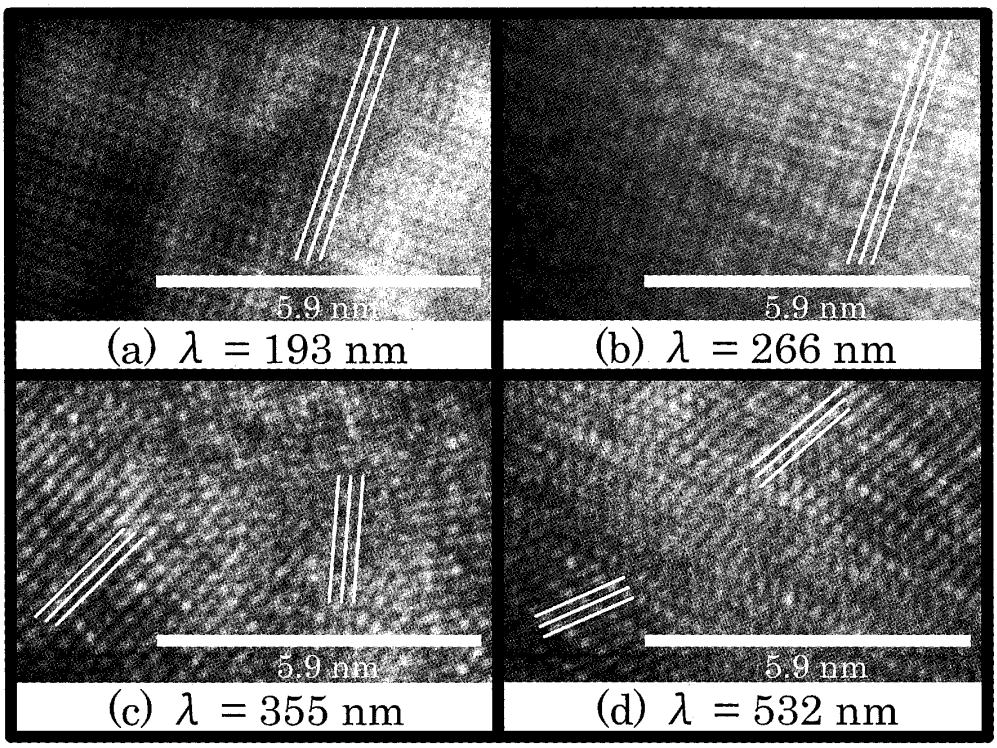

Fig. 5. FE-TEM images of AZO films (100 layers) fabricated with various wavelengths (193-532 nm).

From the above-mentioned results, it was found that the lowest resistivity of 3.64×10^{-4} Ω · cm (Table 2) and the lowest surface roughness of 0.79 nm (Fig. 3) were obtained for the AZO films (approximately 100-nm-thick of 100 layers) deposited with a wavelength of 193 nm. To further increase these values, four parameters other than the laser wavelength, namely, the laser energy density, the repetition frequency, the trace ratio and the number of stacking layers were optimized. These parameters were varied respectively from 2.5 to 1 J/cm^2, 10 to 2 Hz, 1 : 1 to 1 : 4 (equivalent to AZO (1.8 wt.%)) and 100 to 500 layers. For one set of parameters, which are laser energy density of 1 J/cm^2, repetition frequency of 10 Hz, trace ratio of 1 : 4 and 100 stacking layers, $\rho = 2.73 \times 10^{-4}$ Ω · cm, $\mu = 27.2$ cm^2/V · s, the carrier concentration of $n = 8.41 \times 10^{20}$cm^{-3} were obtained for 100-nm-thick AZO films. For another set of parameters, namely, laser energy density of 1 J/cm^2, repetition frequency of 2 Hz, trace ratio of 1 : 4 and 500 stacking layers, $\rho = 2.24 \times 10^{-4}$ Ω · cm, $\mu = 33.4$ cm^2/V · s, the carrier concentration of $n = 8.32 \times 10^{20}$cm^{-3} were obtained for the 100-nm-thick AZO films. As the film thickness is fixed to be approximately 100 nm, each thickness per one layer are estimated 1 nm for the film consisted of AZO(1 wt.%, 50 layers) and AZO(2 wt.%, 50 layers) and 0.2 nm for the film consisted of AZO(1 wt.%, 250 layers) and AZO(2 wt.%, 250 layers). Whereas, the interplaner spacing of ZnO(0002) is 0.26 nm. Therefore, for the

film with large number of layer, the thickness per one layer approaches the interplaner spacing of ZnO(0002). Namely, an optimization of composition ratio toward AZO(1.5 wt.%) was caused. Consequently, the ingredient of aluminum was suitably taken into the lattice of ZnO, leading to the depression of carrier-scattering. From these results, it was considered that the improvement in the electrical properties of the films with 500 stacking layers may be attributed to an optimization of the film composition, which was well inferred from a raise in mobility related to an improvement of crystallinity of the AZO films.

On the other hand, no matter what fabrication conditions were employed, the optical properties of almost all the films showed practically the same average transmittance in the visible range of more than 90 %, which was large enough to fulfill the function of TCO films. Fig. 6 shows the transmittance spectra for the films with 100 and 500 layers for a laser energy density of 1 J/cm^2 and trace ratio of 1 : 4. From this, it was confirmed that with optimization of the laser energy density and the trace ratio, an average transmittance of more than 90 % in the visible range could be obtained for the AZO films with 100 and 500 layers.

Fig. 7 shows FE-SEM and AFM micrographs obtained for the surfaces of AZO films with (a) 100 and (b) 500 layers fabricated with the optimized conditions. From the FE-SEM images, it was difficult to distinguish aspects of the surfaces of the AZO films with 100 and

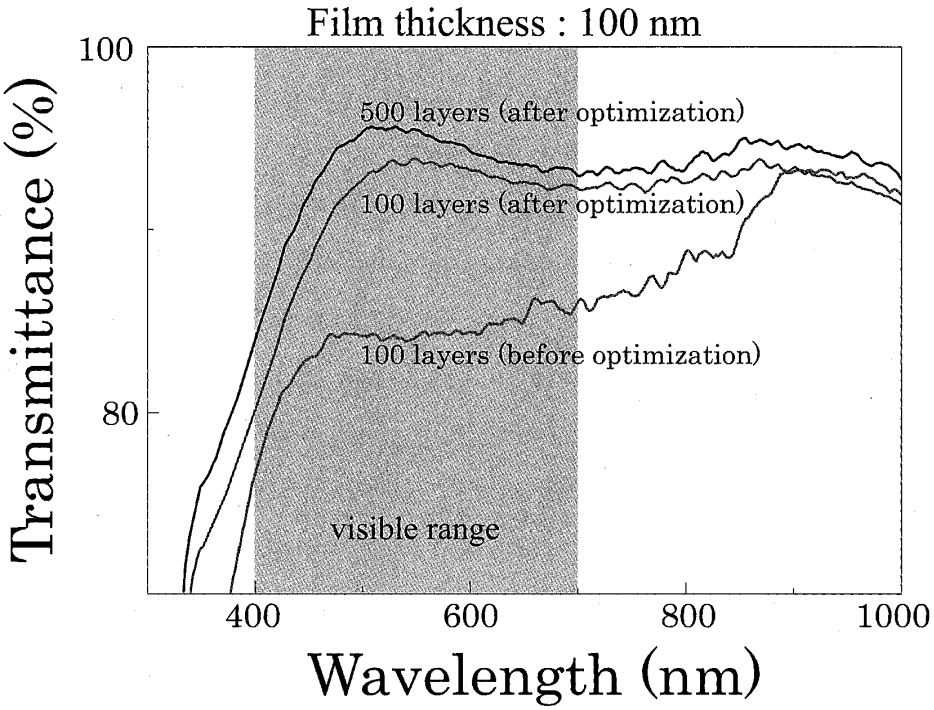

Fig. 6. Transmittance spectra for AZO films with 100 and 500 layers fabricated under optimized conditions of laser energy density 1 J/cm^2 and trace ratio 1 : 4.

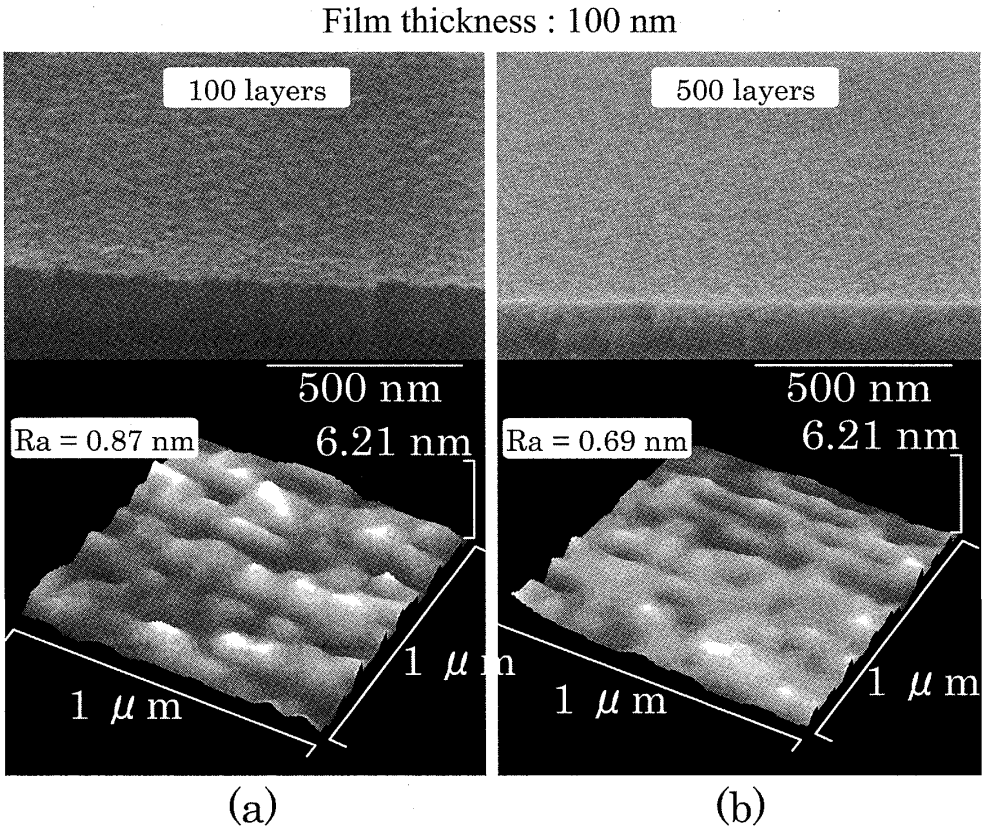

Fig. 7. FE-SEM and AFM micrographs obtained for AZO films with (a) 100 and (b) 500 layers fabricated under optimized conditions.

500 stacking layers from each other. Whereas from the AFM images, it was confirmed that the surface roughness decreased from 0.87 nm in the case of 100 layers to 0.69 nm in the case of 500 layers, namely, an improvement of the morphology on the surfaces was achieved for the films with 500 thin layers. To confirm this result, subsequent XRD measurements and FE-TEM observations were performed. Fig. 8 (a) shows XRD spectra obtained for AZO films fabricated by stacking 100 and 500 layers and Fig. 8 (b) shows FE-TEM images obtained near the interface between the substrate and the films. It was found from Fig. 8 (a) that the ZnO(0002) peak of c-axis orientation for AZO film with 500 stacking layers was nearly twice as high as that for the AZO film with 100 layers. Moreover, it was found that the full width at half maximum (FWHM) value of the ZnO(0002) peak remarkably improved from 1.34° for films with 100 layers to 0.73° for films with 500 layers. Moreover, in the FE-TEM images of Fig. 8 (b) for both 500 and 100 layers, no disarrangement appeared, and a regularity in the crystal growth was propagated toward the film surface, which showed clearly an improvement compared to the result of Fig. 5 (a) obtained under conditions before optimization.

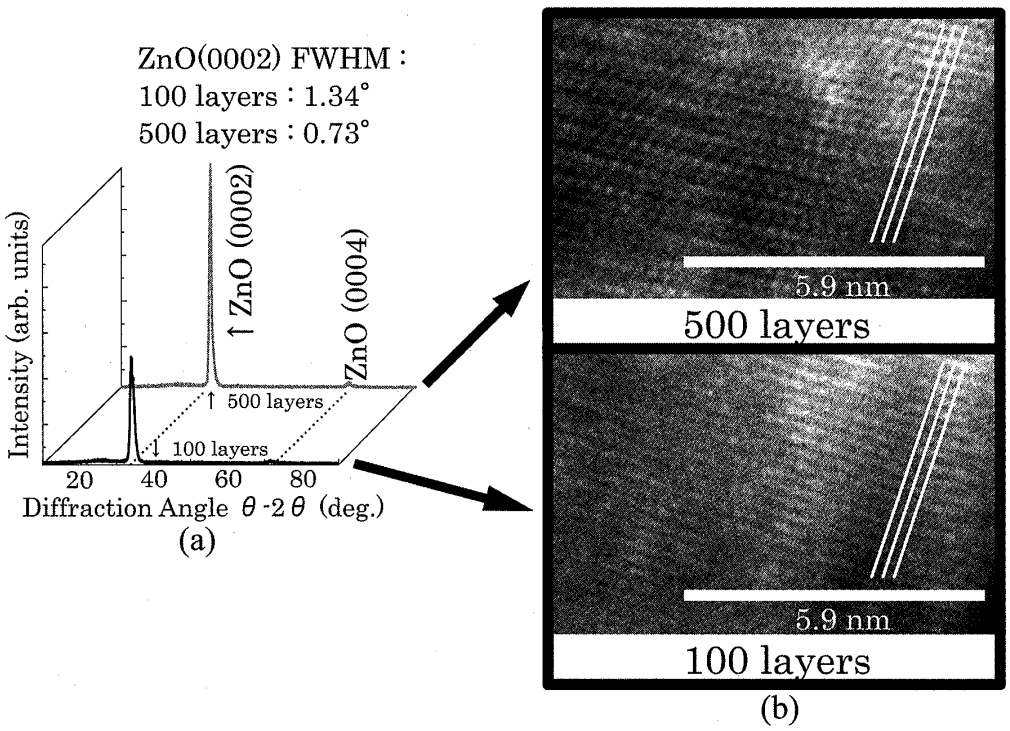

Fig. 8. (a) XRD spectra and (b) FE-TEM images for AZO films with 100 and 500 layers fabricated under optimized conditions.

Conclusions

Approximately 100-nm-thick AZO films with 100-500 stacking layers have been prepared on glass substrates at 230°C by the PLD with the varied wavelengths (λ = 532, 355, 266 and 193nm) using a split target consisted of AZO (1 wt.%) and AZO (2 wt.%), under conditions of laser energy density of 1-2.5 J/cm^2, repetition frequency of 2-10 Hz and trace ratio of 1 : 1-1 : 4.

For AZO film with 500 stacking layers obtained under optimized conditions of laser energy density of 1 J/cm^2, repetition frequency of 2 Hz, trace ratio of 1 : 4, the following results were obtained: (1) The lowest resistivities of 2.73×10^{-4} and $2.24\times10^{-4}\Omega$ · cm were obtained for the films with 100 and 500 layers, respectively. (2) An average transmittance of more than 90 % in the visible range were obtained for the AZO films with 100 and 500 layers, providing useful functionality as TCO films in the visible range. (3) The values of the surface roughness were 0.87 nm and 0.69 nm for the AZO films with 100 and 500 layers, respectively. (4) The values of FWHM of the ZnO(0002) peak were 1.34° and 0.73° for the films with 100 and 500 layers, respectively. These results provide useful functionality as TCO films in the visible range.

References.

[1] S. Hayamizu, H. Tabata, H. Tanaka, T. Kawai, J. Appl. Phys. 80 (1996) 787.

[2] A. Suzuki, T. Matsushita, T. Fukuda, H. Fujiwara, M. Okuda, Trans. IEE. of Japan, 117A (1997) 405.

[3] A. Suzuki, T. Matsushita, T. Aoki, Y. Yoneyama, M. Okuda, Jpn. J. Appl. Phys. 38 (1999) L71.

[4] H. Agura, A. Suzuki, T. Matsushita, T. Aoki, M. Okuda, Thin Solid Films, 445 (2003) 263.

[5] H. S. Kang, J.S. Kang, J.W. Kim, S.Y. Lee, J. Appl. Phys. 95 (2004) 1246.

[6] H. Ohta, M. Orita, M. Hirano, J. Appl. Phys. 89 (2001) 5720.

[7] Y.W. Heo, L. C. Tien, D. P. Norton, B. S. Kang, F. Ren, B. P. Gila, S. J. Pearton, Appl. Phys Lett. 85 (2004) 2002.

[8] Y.W. Heo, L.C. Tien, D. P. Norton, S. J. Pearton, B.S. Kang, F. Ren, Appl. Phys. Lett. 85 (2004) 2274.

[9] A. Valentini, F. Quaranta, M. Penza, F.R. Rizzi, J. Appl. Phys. 73 (1993) 1143.

[10] S. J. Baik, J.H. Jang, C .H. Lee, W.Y. Cho, K.S. Lim, Appl. Phys. Lett. 70 (1997) 3516.

[11] N. Asakuma, H. Hirashima, T. Fukui, M. Toki, K. Awazu, H. Imai, Jpn. J. Appl. Phys. 41 (2002) 3909.

[12] T. Minami, S. Ida, T. Miyata, Y. Minamino, Thin Solid Films, 445 (2003) 268.

[13] S. Shirakata, T. Sakemi, K. Awai, T. Yamamoto, Thin Solid Films, 445 (2003) 278.

[14] Y. F. Lu, H. Q. Ni, Z. H. Mai and Z. M. Ren, J. Appl. Phys. 88 (2000) 498.

[15] T. Minami, T. Miyata, T. Yamamoto, H. Toda, J. Vac. Sci. Technol. A18 (2000) 1584.

[16] C. Agashe, O. Kluth, J. Hupkes, U. Zastrow, B. Rech, J. Appl. Phys. 95 (2004) 1911.

[17] A.V. Singh, R.M. Mehra, A. Yoshida, A. Wakahara, J. Appl. Phys. 95 (2004) 3640.